

# A Comparison of the Firing Properties of Putative Excitatory and Inhibitory Neurons From CA1 and the Entorhinal Cortex

LOREN M. FRANK,<sup>1,2</sup> EMERY N. BROWN,<sup>2</sup> AND MATTHEW A. WILSON<sup>1</sup>

<sup>1</sup>Center for Learning and Memory, RIKEN-MIT Neuroscience Research Center and Department of Brain and Cognitive Sciences, Massachusetts Institute of Technology, Cambridge 02139; and <sup>2</sup>Neuroscience Statistics Research Laboratory, Department of Anesthesia and Critical Care, Massachusetts General Hospital and Harvard Medical School/MIT Division of Health Sciences and Technology, Boston, Massachusetts 02114

Received 16 January 2001; accepted in final form 21 May 2001

**Frank, Loren M., Emery N. Brown, and Matthew A. Wilson.** A comparison of the firing properties of putative excitatory and inhibitory neurons from CA1 and the entorhinal cortex. *J Neurophysiol* 86: 2029–2040, 2001. The superficial layers of the entorhinal cortex (EC) provide the majority of the neocortical input to the hippocampus, and the deep layers of the EC receive the majority of neocortically bound hippocampal outputs. To characterize information transmission through the hippocampal and EC circuitry, we recorded simultaneously from neurons in the superficial EC, the CA1 region of hippocampus, and the deep EC while rodents ran for food reward in two environments. Spike waveform analysis allowed us to classify units as fast-spiking (FS) putative inhibitory cells or putative excitatory (PE) cells. PE and FS units' firing were often strongly correlated at short time scales, suggesting the presence a monosynaptic connection from the PE to FS units. EC PE units, unlike those found in CA1, showed little or no tendency to fire in bursts. We also found that the firing of FS and PE units from all regions was modulated by the ~8 Hz theta rhythm, although the firing of deep EC FS units tended to be less strongly modulated than that of the other types of units. When we examined the spatial specificity of FS units, we determined that FS units in all three regions showed low specificity. At the same time, retrospective coding, in which firing rates were related to past position, was present in FS units from all three regions and deep EC FS units often fired in a "path equivalent" manner in that they were active in physically different, but behaviorally related positions both within and across environments. Our results suggest that while the firing of FS units from CA1 and the EC show similarly low levels of position specificity, FS units from each region differ from one another in that they mirrored the associated PE units in terms of their tendency to show more complex positional firing properties like retrospective coding and path equivalence.

## INTRODUCTION

The hippocampal formation has long been known to be important in rodents' abilities to learn and remember spatial tasks (Jarrard 1993; O'Keefe and Nadel 1978; Whishaw and Tomie 1991) and units (putative single neurons) throughout the hippocampal formation have been shown to be active in a place-specific manner when a rodent moves through its environment (Barnes et al. 1990; Jung and McNaughton 1993; McNaughton et al. 1983; Muller 1996; Muller et al. 1994; O'Keefe and Dostrovsky 1971; Sharp 1997). The superficial

layers of the entorhinal cortex (EC) provide the majority of the neocortical input to the hippocampus and the deep layers of the EC receive the majority of neocortically bound hippocampal outputs (Amaral and Witter 1995; Witter et al. 1989), but despite its close anatomical relationship to hippocampal structures, the EC has received less attention than the hippocampus. Those studies that have been done suggest that the EC is important to an animal's ability to perform both spatial (Cho and Jaffard 1994; Cho and Kesner 1996; Hagan et al. 1992; Holscher and Schmidt 1994; Johnson and Kesner 1994; Nagahara et al. 1995; Rasmussen et al. 1989) and nonspatial tasks (Izquierdo and Medina 1993; Izquierdo et al. 1997; Sutherland et al. 1989; Vnek et al. 1995).

Earlier work that examined the spatial firing properties of EC neurons suggested that cells in both the superficial and deep EC fire with less spatial specificity than hippocampal cells (Barnes et al. 1990; Mizumori et al. 1992; Quirk et al. 1992). More recently, we reported results from simultaneous recordings from CA1 and the EC in animals running on both a W- and a U-shaped track (Frank et al. 2000). We found that deep EC units showed significantly more spatial specificity than superficial EC units but less than CA1 units. Deep EC units also showed a strong tendency to be active at the same relative location along different paths through the environment, a tendency we termed "path equivalence." We also found that cells throughout the EC and CA1 can fire differently in the same location depending on where the animal has just been or is intending to go, and thus that these cells can code retrospectively (for past location) or prospectively (for future location).

Results from studies of the hippocampus and neocortical areas suggest that spike waveform shape can be used to distinguish between putative excitatory (PE) cells from putative inhibitory or fast spiking (FS) interneurons (Brumberg et al. 1996; Csicsvari et al. 1999; Fox and Ranck 1981; Kyriazi et al. 1996; McCormick et al. 1985; Rao et al. 1999; Simons 1978; Swadlow 1995; Swadlow et al. 1998; Wilson et al. 1994). In the hippocampus, PE and FS cells have fundamentally different spatial and nonspatial firing properties (Fox and Ranck 1981; Kubie et al. 1990; McNaughton et al. 1983). The divi-

Address for reprint requests: M. A. Wilson, E18-370, 45 Carleton St., MIT, Cambridge, MA 02139 (E-mail: wilson@ladyday.mit.edu).

The costs of publication of this article were defrayed in part by the payment of page charges. The article must therefore be hereby marked "advertisement" in accordance with 18 U.S.C. Section 1734 solely to indicate this fact.

sion of cells into PE and FS subtypes has not been performed in the EC.

Here we use spike waveform shape and average firing rate to distinguish between putative interneurons and excitatory cells recorded from animals that ran on both a W-shaped and a U-shaped track. We then examined their firing patterns to characterize unit activity in CA1 and the EC with respect to spike train properties like interspike interval distributions and with respect to spatial specificity. Analyses on the same data that focused on prospective and retrospective coding and path equivalence have been presented elsewhere (Frank et al. 2000).

## METHODS

### Subjects

The data presented here are from four Long-Evans rats (Charles River Laboratories) that were between 3 and 6 mo of age at the time of surgery.

### Microdrive array construction

The microdrive array consisted of a total of 20 independently movable microdrives each controlling the depth of an individual tetrode. Each tetrode consisting of four 12.5- $\mu\text{m}$ -ID polyamide-insulated nichrome wires. The microdrive array advanced the tetrodes through two large cannulae, one oriented vertically that targeted the CA1 region of the hippocampus and the other angled laterally outwards at 9° from the vertical in the transverse plane targeting the EC. A total of 7 tetrodes targeted CA1 and a total of 13 tetrodes targeted the EC. Single hippocampal and EC tetrodes were used as local reference electrodes for the hippocampus and EC respectively.

### Surgical procedures

Once trained (see *Behavioral methods*), each animal was anesthetized intraperitoneally with a mixture of ketamine (50 mg/kg) and xylazine (6 mg/kg) and maintained on isoflurane (0.5–2.0%). The animal was given a local injection of 0.2 ml lidocaine subcutaneously to the scalp, and atropine (0.1 mg/kg ip). In addition, the animal was given three injections of monophosphate sodium succinate (30 mg/kg), one before the dura removal and two more spaced ~30–45 min thereafter in a protocol adapted from (Behrmann et al. 1994). A total of 11–13 screw holes were drilled and small bone screws were inserted. One of these screws, usually positioned in the most anterior position over the left hemisphere, was used as a ground. Two holes were drilled in the bone covering the right hemisphere for the microdrive array, one at AV –3.6, L 2.2 for the electrodes targeting CA1 and the other at AV –7.8, L 4.8 for the electrodes targeting the EC. The microdrive array was then affixed to the skull with dental acrylic. In some cases the animal appeared dehydrated after surgery so between 5 and 10 ml of warm Ringer solution were injected subcutaneously.

### Behavioral methods

The behavioral methods have been presented elsewhere (Frank et al. 2000). The animals were trained to run on a U-shaped track and on a W-shaped track (Fig. 1) for a reward of powdered hot-chocolate mix mixed with water. On the U track, the animal performed a simple alternation task, whereas on the W track, the animal was placed on the center arm and then trained to run in an alternation task from center to left to center to right to center arms and so on.

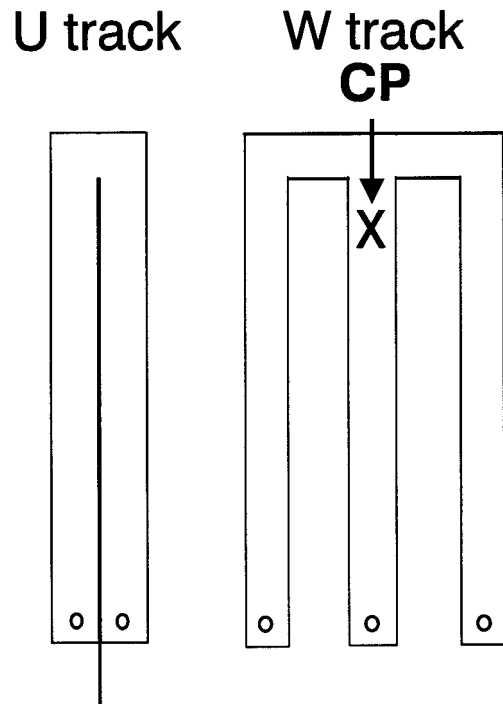


FIG. 1. The W- and U-track environments. These 2 environments were located next to each other in the recording room and oriented as shown in the figure. The tracks were 150 cm along their longest dimension, and the W track was a total of 49 cm wide, whereas the U track was ~15 cm wide. The distance between the edges of the 2 tracks was ~20 cm, and the individual track sections that the animal ran on were 7 cm wide.

### Recording techniques and procedures

The recording apparatus consisted of three custom-made 25-channel preamplifier chips that were attached to connectors on the top of the microdrive array, a set of 11 eight-channel amplifiers (DataWave), a set of 12 synchronized 486–100 PCs running the AD software package (M. Wilson and L. Frank), and a tracking system (Tracker SA-W, Dragon, Boulder, CO). Signals from the four electrodes of a tetrode were amplified between 10,000 and 40,000 times and, for spike waveforms, filtered between either 300 Hz and 6 kHz (EC) or between 600 Hz and 6 kHz (CA1). The difference in low cutoff was used because some entorhinal spikes were quite wide and were thus excessively attenuated by the 600-Hz cutoff. The spike data were sampled at 31.25 kHz per channel. Whenever the signal from one electrode on a tetrode exceeded a threshold set by the experimenter, a 1.02-ms (32 point) window of data from each of the four electrodes was stored to disk. One channel from each of 16 tetrodes was chosen for electroencephalography (EEG). The signal from this channel was amplified 2,000 times, filtered between 1 Hz and 475 Hz, sampled at 1.5 kHz per channel, and stored to disk. Position tracking was done with the aid of two infrared diode arrays mounted on a boom attached to the preamplifier chips. The boom was positioned so that when the animal ran, the front diode array was located slightly in front of the animal's nose and the rear array was over the back of the animal's neck. The positions of the diodes were saved to disk at 30 Hz.

After the surgery, the animal was brought to the recording room, and the tetrodes were slowly advanced into the brain over the next 5–7 days. Histological analysis later revealed that the EC reference electrode was in all cases either in the deep layers of the superficial cortex near the angular bundle or in the bundle itself. Once the EC electrodes were in or near the deep layers of the EC, recording sessions were begun. The animal was brought up from the animal facility and placed in the sleep box, and, if necessary, each of the tetrodes was adjusted by between 20 and 160  $\mu\text{m}$  to maximize the number of cells visible.

Whenever possible electrodes were adjusted only after the recording session to maximize recording stability. In the case of the hippocampal tetrodes, the movement was either up or down depending on the tetrode's location with respect to the cell layer. The entorhinal electrodes were always moved downward to help guarantee that the same cells were not recorded from twice. That meant that initial recordings were in the deep layers of the EC and later recordings were in progressively more superficial layers. After adjusting, the electrodes were allowed to settle for ~2 h. The recording session was then begun and the behavioral protocol described in the preceding text was followed.

### Histological analysis

The histological methods have been presented elsewhere (Frank et al. 2000). Briefly, each EC tetrode was used to make between one and four lesions. To reconstruct the positions of each of the tetrodes, the relative locations, the number of lesions made, and the final depth of each tetrode was used to determine which electrode tracks corresponded to which tetrodes. The tetrode was then assigned a location for each day of recording. If a tetrode's location could not be determined with a high degree of confidence, data from that tetrode were not used.

### Data analysis

After each recording session, the data were transferred to a Linux workstation for analysis. A custom software package (Xclust, M. Wilson) was used to cluster the spike waveforms from each tetrode into putative single neurons, hereafter termed single units. All other analyses were carried out using custom software written in the Matlab (MathWorks, Natick, MA) environment. For each tetrode in CA1, we examined the spatial firing properties of every cell from that tetrode, and, for each cell that was recorded from across multiple data sets, we included the data from only one of the data sets in our analyses. Only data from the run periods of the recording are examined here and only those units with at least one place field (see following text) and for which <5% of the interspike intervals were <3 ms were included in the analyses. We also eliminated all units with average amplitude of <70  $\mu$ V.

In addition, as we wished to examine the very short time scale (0–5 ms) cross-correlations of pairs of units, we examined all pairs of CA1 units recorded from the same tetrode with a significant peak in the cross-correlogram between 0 and 5 ms. Quirk and Wilson (1999) demonstrated that because CA1 principal cells tend to fire complex spike bursts where the amplitude of each subsequent spike decreases as compared with the first spike, even very slight errors in clustering can result in fictitious correlations between pairs of units. As such, for all CA1 unit pairs with a significant correlation ( $P < 0.001$ , see following text for cross-correlation definition and significant tests), we calculated a complex spike index (CSI) that estimates the percentage of spikes from one unit that follow the spikes of another unit within a 10-ms interval and are of lower amplitude (McHugh et al. 1996). For those unit pairs with a CSI >3.0, we eliminated the unit with the lower amplitude spikes.

**UNIT CLASSIFICATION.** We characterized the waveform shapes of each unit by computing the width of the waveform defined as the mean absolute value of the time from the peak to the trough of the units' spikes. We then used the resulting distributions of widths, combined with the average rate of the units, to classify each CA1 unit as either a PE unit or a FS unit and to classify each EC unit as either PE or FS. The criteria used and their justification are presented in RESULTS. This terminology was chosen to reflect on one hand the general use of the term "fast-spiking" to refer to putative interneurons with narrow spike waveforms (Brumberg et al. 1996; McCormick et al. 1985; Rao et al. 1999; Simons 1978; Wilson et al. 1994) and, on the other hand, the diversity of excitatory subtypes present in the EC.

We should note, though, that our definition of spike width is different from that used by others who measured the time from the inflection point marking the initial negativity to the time when the waveform returned to baseline (Rao et al. 1999; Wilson et al. 1994). Our software stored each spike in a 1.02-ms window, and the waveforms often did not return to baseline within that window. As such, the full width of the waveform was not available to us. Also, note that Kyriazi et al. (1996) proposed a somewhat different set of criteria where PE and FS cells were separated by computing the product of the 10–90% rise time of the positive peak of the waveform and the width of this peak at half height. In our case, the peak-to-trough width of EC waveforms was clearly bimodal, whereas the width of the waveform peak at half height was not clearly bimodal, so the criterion based on peak to trough waveform width appeared to be most appropriate.

**CROSS-CORRELATION ANALYSIS.** Previous work has shown that the cross-correlation of CA1 PE and FS units often has a peak at 1–3 ms suggestive of a monosynaptic excitatory connection from PE to FS units (Csicsvari et al. 1998). To examine whether that coupling is found not only in CA1 but also in the EC, we examined the cross-correlation of all pairs of units recorded simultaneously from the same tetrode. To compute the cross-correlation, we employed the techniques proposed by Brillinger (1976). This approach allows for a simple computation of confidence bounds without the need to shuffle the spike trains. To compute the cross-correlation between units A and B, two normal cross-correlation histograms are constructed with the desired bin size, the A versus B cross-correlation histogram using the spikes of B as the  $t = 0$  reference point and the B versus A cross-correlation histogram using the spikes of A as the  $t = 0$  reference point (Perkel et al. 1967). For the first histogram (A vs. B) each bin of the histogram is then subjected to the following variance normalizing transformation:  $\text{newbin}(i) = \sqrt{\text{bin}(i)/(\text{binsize} \times \text{nspikes}_B)}$  where  $\text{newbin}(i)$  is the new value for the bin,  $\text{bin}(i)$  is the original value for the bin,  $\text{binsize}$  is the size of the bin, and  $\text{nspikes}_B$  is the number of spikes fired by cell B. The counts in each bin are thereby transformed to be approximately normal, and a mean and 95% confidence bound can then be calculated as follows:  $\text{mean} = \sqrt{\text{nspikes}_A/\text{totaltime}}$  95%;  $\text{confbound} = \text{mean} \pm \sqrt{1/(\text{binsize} \times \text{nspikes}_B)}$  where  $\text{totaltime}$  is the total length of the recording period. As the value in each bin is approximately normal, any other confidence bound can be derived by multiplying the 95% bound by the ratio of the  $z$  score of the desired bound to that of the 95% bound (i.e., desired  $Z/1.96$ ). The same equations are used for the B versus A histogram with the A and B indices switched. As we were interested in determining which pairs of neurons showed a strong very short latency (0–3 ms) peak in their correlogram, we used a confidence interval of  $P < 0.001$  and calculated the cross-correlations between –30 and 30 ms with a bin size of 1 ms. In addition, as rhythmic modulation of cell pairs could result in a broad peak of the correlogram that extended over the 1- to 5-ms range, we recalculated a local mean value as the mean of the cross-correlogram in the two intervals from 5 to 25 ms from  $t = 0$  (i.e., –25 to –5 and 5 to 25). That prevented broad peaks from being considered significant. The cross-correlations of a pair of units was considered to be significant if either the A versus B or B versus A correlogram had a peak between 1 and 5 ms that exceeded the local mean plus the confidence interval.

**SPIKE TRAIN CHARACTERISTICS.** To determine whether the previously observed differences in spatial coding seen among the superficial EC, CA1, and the deep EC are associated with differences in firing patterns in the PE or FS units from those regions, we examined three characteristics of the spike trains from these units: the interspike interval distributions, autocorrelation histograms, and the proportion of spikes belonging to bursts. We calculated the proportion of spikes belonging to bursts for each unit by finding the proportion of spikes associated with interspike intervals of <10 ms (Buzsaki et al. 1996).

**THETA MODULATION.** As the activity of CA1 PE and FS units is strongly modulated by the  $\sim 8$ -Hz theta rhythm (Buzsaki and Eidelberg 1983), we also investigated the relationship between theta and unit activity in the EC. To examine that relationship, we selected, for each day of recording from each animal, the EEG signal from one tetrode located in the deep EC, band-pass filtered the EEG between 6 and 14 Hz, and resampled the resulting signal at 200 Hz. A single tetrode was chosen because previous work has demonstrated that hippocampal and entorhinal theta are highly coherent (Alonso and Garcia-Austt 1987a; Chrobak and Buzsaki 1998), so while theta recorded from different electrodes will have different relative phases, the signals have a constant phase relationship to each other. We used a simple peak finding algorithm to determine the locations of the peaks of theta. Each peak was assigned a phase of  $0^\circ$  and the phase of the theta rhythm between peaks was determined by linear interpolation.

We then determined the phase of theta at the time of each spike from each unit. To calculate the degree of theta modulation for each unit, we constructed a histogram of the number of spikes in each of 30 phase bins and smoothed the resulting histogram with a seven point Gaussian filter with a standard deviation of one. That smoothing was performed by convolving the Gaussian with the histogram and removing the three  $[(7-1)/2]$  extraneous points generated by the convolution from each side of the resulting signal. The smoothing was designed to reduce the magnitude of artifacts caused by binning the data. We normalized the resulting histogram by its maximum value and determined the degree of theta modulation by the difference between the maximum and minimum values of the histogram (i.e., theta modulation coefficient =  $1 - \text{minimum value}$ ).

**SPATIAL FIRING PROPERTIES.** Our previous analyses of spatial specificity did not separate PE and FS units, so we examined the spatial specificity of PE and FS units from the superficial EC, CA1, and the deep EC to determine how the differences in place specific firing were previously observed (Frank et al. 2000) were expressed in different types of units. To do so, we employed the same approach used in the previous manuscript. Briefly, we examined the firing of each unit along the paths between food wells. For the W track, the four paths the animal ran along were examined (center to left arm, left to center arm, center to right arm, and right to center arm), while for the U track, two paths (left to right arm and right to left arm) were examined. We linearized each of those paths and determined the distance from the start food well of the path to each linearized position, resulting in a set of positions versus over the distance from the beginning of the path for each path. We binned those distances into 4.2 cm bins and smoothed the result with a six-point Gaussian window with a standard deviation of one.

We analyzed the activity of each unit along each path by computing three related measures of position specificity: average field size, proportion of the environment covered by fields, and position information. We defined a "place field" as described in Frank et al. (2000). Average field size was computed as the mean of the lengths of all fields for each unit, and the proportion of the environment covered by a unit's fields was computed as the total length of the unit's fields along all paths divided by the total length of the paths. Position information was calculated as the number of bits/spike, treating each path as a separate set of locations according to the formula of Skaggs et al. (1993).

**PROSPECTIVE AND RETROSPECTIVE CODING.** In previous work (Frank et al. 2000), we found that the firing of some superficial EC, CA1, and deep EC showed prospective or retrospective coding and that deep EC units were most likely to show prospective coding. We extended those analyses by determining whether both PE and FS units can show these properties and whether the same increase in the prevalence of prospective coding seen from CA1 to the deep EC was present in both PE and FS units. The methods associated with these

analyses are the same as those presented in the previous manuscript (Frank et al. 2000).

**PATH EQUIVALENCE.** We have also previously noted that many deep EC units fired in a path equivalent manner, where units were active at the same relative location along multiple paths both within the W track and between the W and U tracks while CA1 PE units did not fire in a path equivalent manner (Frank et al. 2000). Here we extend those analyses to determine whether the same differences are present in both PE and FS units. The methods associated with these analyses are the same as those presented in the previous work where we computed a path equivalence coefficient to measure the extent to which a unit fired in the same relative location along different paths.

## RESULTS

After histological reconstruction of the electrode and analysis of place firing properties, we determined that the total number of units with place fields was as follows: W track: 36 superficial EC, 308 CA1, and 174 deep EC units; U track: 34 superficial EC, 348 CA1, and 150 deep EC units; both environments: 15 superficial EC, 136 CA1, and 90 deep EC units. Based on the histology, we believe that most of the superficial EC units were recorded from layer 3. The firing properties of units were generally similar in the two environments, so for the moment we focus on the data from runs on the W track.

### *Unit classification*

CA1 units can be divided into two categories: principal units (putative pyramidal cells, hereafter referred to as PE units) and theta units (putative interneurons, hereafter referred to as FS units), distinguishable by the width of the waveforms, interspike interval characteristics and firing rates (Fox and Ranck 1981). Using those criteria, we determined that of the 308 CA1 units, 20 were fast spiking (FS) units. As FS units can be distinguished from PE units on the basis of their narrow spike waveform widths and high average firing rates (Brumberg et al. 1996; McCormick et al. 1985; Rao et al. 1999; Simons 1978; Swadlow et al. 1998; Wilson et al. 1994), we examined the distributions of average firing rates and the relationship between waveform width and average rate (see Fig. 2, A and B). An examination of those relationships indicated that, for both superficial and deep EC units, there is one clear group of units with lower average firing rates ( $< 16$  Hz) and wide waveforms ( $> 0.4$  ms). We classified those units as PE units (shown as "+"s in Fig. 2, A and B, deep EC  $n = 140$ ; superficial EC  $n = 28$ ).

Of the remaining narrow waveform ( $< 0.4$  ms) units, there was a wide distribution of average rates. As FS units are generally associated with high firing rates, we classified only those units with narrow waveforms and average rates  $> 16$  Hz as FS units (shown as triangles in Fig. 2, A and B, deep EC  $n = 16$ ; superficial EC  $n = 6$ ). Those units with narrow waveforms and low average rates are difficult to classify, as they do not obviously correspond to a known EC cell type. As such, we chose to exclude these units from our analyses (shown as  $\circ$  in Fig. 2, A and B, deep EC  $n = 18$ ; superficial EC  $n = 2$ ). We should note that it is likely at least some of these units corresponded to FS cells, as our rate cutoff for inclusion in the FS unit group is high. Furthermore, an examination of those units with narrow spike widths and low average firing rates ( $< 5$  Hz) suggested that these units had positional firing properties sim-

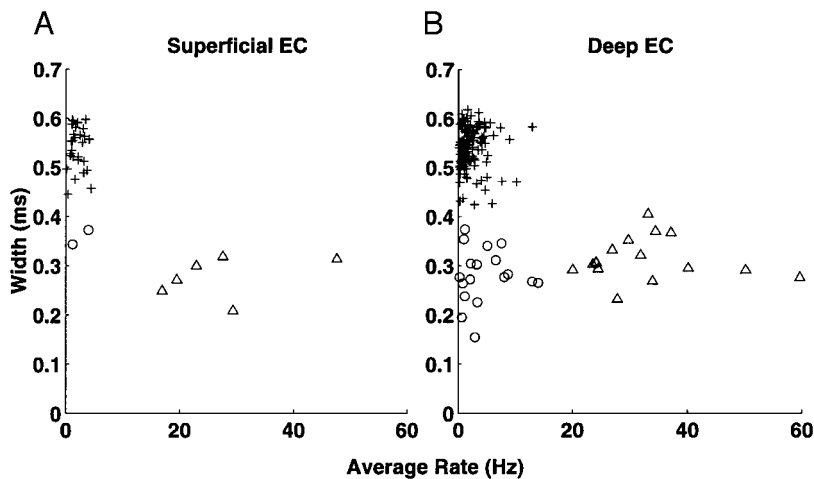


FIG. 2. Classification of units into putative excitatory (PE) and fast spiking (FS). *A* and *B*: scatter plots of the relationship between waveform width and average rate for superficial and deep EC units, respectively. Units with wide waveforms tended to fire at lower average rates. +, PE units;  $\Delta$ , FS units.  $\circ$ , units excluded from the analyses because they were not clearly PE or FS units.

ilar to PE units. Nonetheless, as we wished to compare the firing of PE and FS units, we believe that the exclusion of these units is warranted. The resulting means  $\pm$  SD of the waveform widths for the EC units were as follows: EC FS  $0.30 \pm 0.05$  ms; EC PE  $0.54 \pm 0.04$  ms. The average rate for each type of unit from each region are shown in Table 1. Examples of representative average waveforms from superficial and deep EC PE and FS units are shown in Fig. 3.

Our choice of classification criteria was based solely on the waveform width and average rate of units with fields on the W-track apparatus. If this classification is reasonable, we would expect it to be consistent across environments. That would imply that, for those units with fields in both environments, the average rates of the units would be consistent across the environments and waveform widths would remain relatively constant. Referring for the moment to the cell type classification from the W track, 36 CA1 FS and 158 CA1 PE units, 9 EC FS units (1 from superficial EC, 8 from deep EC), and 87 EC PE units (11 from superficial EC and 76 from deep EC), units had fields in both environments. Of those units, three EC units had inconsistent classifications on the two tracks, all of which were the result of the unit being classified as an PE or FS unit in one environment and one of the narrow waveform, low average rate units (the category we excluded from the analysis) in the other environment. No units were classified as PE in one environment and FS in the other, indicating that the classification was consistent.

#### Cross-correlation analysis

For superficial EC, only 1 PE-FS pair and 13 PE-PE pairs were recorded from, and none of these pairs had a significant short time cross-correlation. An example of the two cross-correlograms from one deep EC PE –FS pair showing strong

coupling is shown in Fig. 4. In CA1, 22% (29 of 107) of the PE-FS pairs but <2% (14 of 814) of the PE-PE pairs had a significant short time cross-correlation. Similarly, in the deep EC, 29% (6 of 21) of the PE-FS pairs and 5% (4 of 75 PE-PE) pairs had a significant short time cross-correlation. Those proportions were significantly different for both CA1 and deep EC units ( $P < 0.01$ , GLM model – binomial link function,  $\chi^2$  test), indicating that for both CA1 and the deep EC, PE-FS pairs were much more likely to show a strong short time scale cross-correlation than PE-PE pairs.

#### Spike train characteristics

The examination of spike train characteristics revealed that FS units had similar characteristics across all regions while PE units tended to differ between CA1 and the EC. An analysis of the interspike interval distributions and average rates indicated that there were no clear differences between superficial EC FS and deep EC FS units or between superficial EC PE and deep EC PE units, so EC FS and EC PE units were each treated as a single group for these analyses. An examination of the interspike interval (ISI) properties of representative units from CA1 and the EC (see Fig. 5*A*) revealed that CA1 FS and EC FS units both tended to fire with an ISI of  $\sim 10$ – $100$  ms, whereas CA1 PE units tended to fire in bursts with very short ISIs. The ISIs of superficial and deep PE units, on the other hand, tended to peak at  $\sim 100$  ms. In some EC FS and PE units and in most CA1 PE units, a peak in the ISI at  $\sim 125$  ms was present, corresponding to the period of the theta rhythm. The normalized autocorrelation histograms of these same units are shown in Fig. 5*B*. The main difference among the plots, aside from the height of the baseline, is the degree of theta modulation ( $\sim 8$  Hz) visible. The autocorrelation histogram of the CA1 PE unit shows very strong theta modulation, while that of the EC PE

TABLE 1. Spike train variables

	Superficial EC FS	Superficial EC PE	CA1 Theta	CA1 PE	Deep EC FS	Deep EC PE
Average rate, Hz	$27.3 \pm 11.0$	$2.0 \pm 1.2$	$31.5 \pm 11.7$	$1.1 \pm 1.1$	$32.6 \pm 10.4$	$2.2 \pm 2.0$
Proportion of bursts	$0.33 \pm 0.16$	$0.08 \pm 0.10$	$0.38 \pm 0.15$	$0.51 \pm 0.15$	$0.22 \pm 0.14$	$0.08 \pm 0.06$
Theta modulation	$0.53 \pm 0.17$	$0.54 \pm 0.14$	$0.59 \pm 0.23$	$0.57 \pm 0.20$	$0.29 \pm 0.16$	$0.51 \pm 0.18$

The mean  $\pm$  SD of the spike train variables measured for each unit type within each region for units with fields on the W track. The rows give the values for average rate, proportion of spikes associated with bursts, and degree of theta modulation associated with each type of unit. EC, entorhinal cortex; FS, fast spiking; PE, putative excitatory.

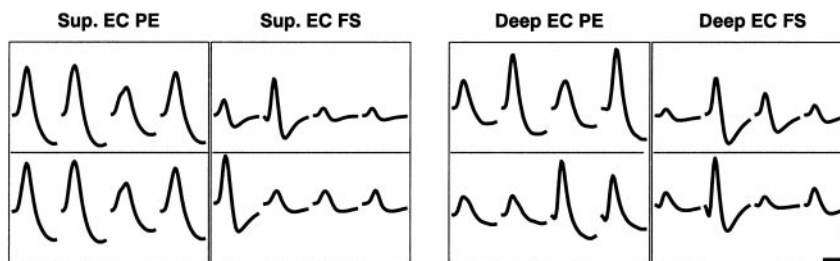


FIG. 3. Examples of PE and FS units recorded from the superficial and deep entorhinal cortex (EC). Each set of 4 traces represents the average amplitude of a single unit across the 4 channels of a tetrode. Spikes from EC PE units tended to be very wide and, for the larger amplitude spikes, the waveform generally did not return to baseline within the 1.02-ms window used for data collection. In contrast, spikes from EC FS units generally returned to baseline within the window. Example spikes from CA1 PE and FS units are not shown because the signals from these units were filtered at a low cutoff frequency of 600 Hz as compared with 300 Hz for the EC cells. As such our data do not permit a direct comparison of the waveform shapes of CA1 and EC units. Scale bars: 0.5 ms and 50  $\mu$ V.

units shows virtually none. Despite those apparent differences, however, the actual degree of theta modulation in the theta histograms shown in Fig. 5C is approximately the same for the units, indicating that the autocorrelogram should not be used to determine whether a unit is or is not rhythmically modulated, a result previously reported by Garcia-Sanchez et al. (1978). Figure 5D shows an example of a raw EEG trace from the reference deep EC electrode and a representative autocorrelogram of the filtered theta rhythm. As expected, the EEG traces and the autocorrelogram show robust theta.

To determine whether variability in theta frequency could account for the apparent lack of theta rhythmicity seen in some EC PE units' autocorrelation histograms, we calculated the mean and standard deviation of theta frequency and found that the mean was  $9.5 \pm 2.9$  Hz. That variability may have contributed to the differences seen in the autocorrelation histograms, but as sets of CA1 and EC units were recorded simultaneously and therefore subjected to identical theta variability,

we believe that variability in theta frequency alone is unlikely to account for the autocorrelation differences.

The proportion of bursts (ISIs <10 ms) for each type of unit is given in Table 1. FS units from all three regions showed a similar tendency to fire spikes within short ISIs. PE units were much less homogeneous, however, as CA1 PE units frequently fired in bursts while both superficial and deep EC PE units seldom fired spikes within short interspike intervals. All of the means were significantly different (Scheffé *S* test,  $P < 0.05$ ) except as follows: the proportion of spikes associated with bursts for superficial EC FS units was not different from that of CA1 FS or deep EC FS units and the proportion of spikes associated with bursts for superficial EC PE and deep EC PE units did not differ. Overall, FS units from the three regions had similar spike train properties but CA1 PE units differed markedly from EC PE units.

#### Theta modulation

The overall distributions of the degree of theta modulation for the different types of units are shown in Fig. 6. Units from all regions showed theta modulation. In addition, the distributions of modulation depths for both superficial EC FS and CA1 FS units appeared to be bimodal, although the number of units was relatively small so no firm conclusions concerning bimodality can be reached. Deep EC FS units were less theta modulated than all other categories of units (Scheffé *S* test,  $P < 0.01$ ), but none of the other FS or PE units differed from any other. Table 1 gives the means  $\pm$  SD for the degree of theta modulation of PE and FS units from the different regions.

#### Spatial firing properties

The spatial firing patterns of EC FS and CA1 FS units were, like their waveforms and ISIs, generally similar. Figure 7 shows the activity of two superficial EC FS units, two CA1 FS units, and two deep EC FS units that had fields in both the W- and the U-track environments. Each row of these figures depicts one unit on each of the four paths of the W track and the two paths of the U track. The FS units tended to be active over large portions of the environment, but their firing rates were clearly higher on some parts of the environment than on others.

The mean field size, proportion of the environment covered by fields, and position information for each type of unit from each region are shown in Fig. 8. The results for PE units are

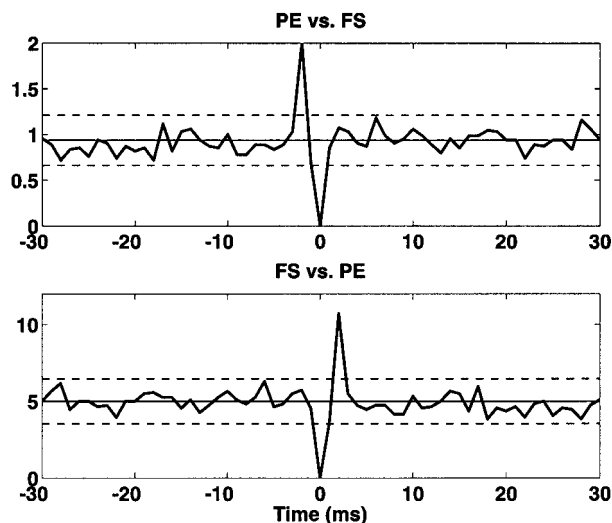


FIG. 4. An example of a high short-time cross-correlation between a deep EC PE and FS unit recorded simultaneously from the same tetrode. The bin size used was 1.0 ms. —, the short time scale mean (the average of the cross-correlation values between  $-25$  and  $-5$  and between  $5$  and  $25$  ms); ---, the  $P < 0.001$  confidence intervals. There is a clear peak visible in both plots showing that spikes from the PE unit preceded spikes from the FS unit at a level far beyond that expected by chance. The dip in the cross-correlation at  $t = 0$  is a result of the 1-ms window used for acquisition where only one spike can be detected in each window and is therefore not indicative of actually firing characteristics of the units.

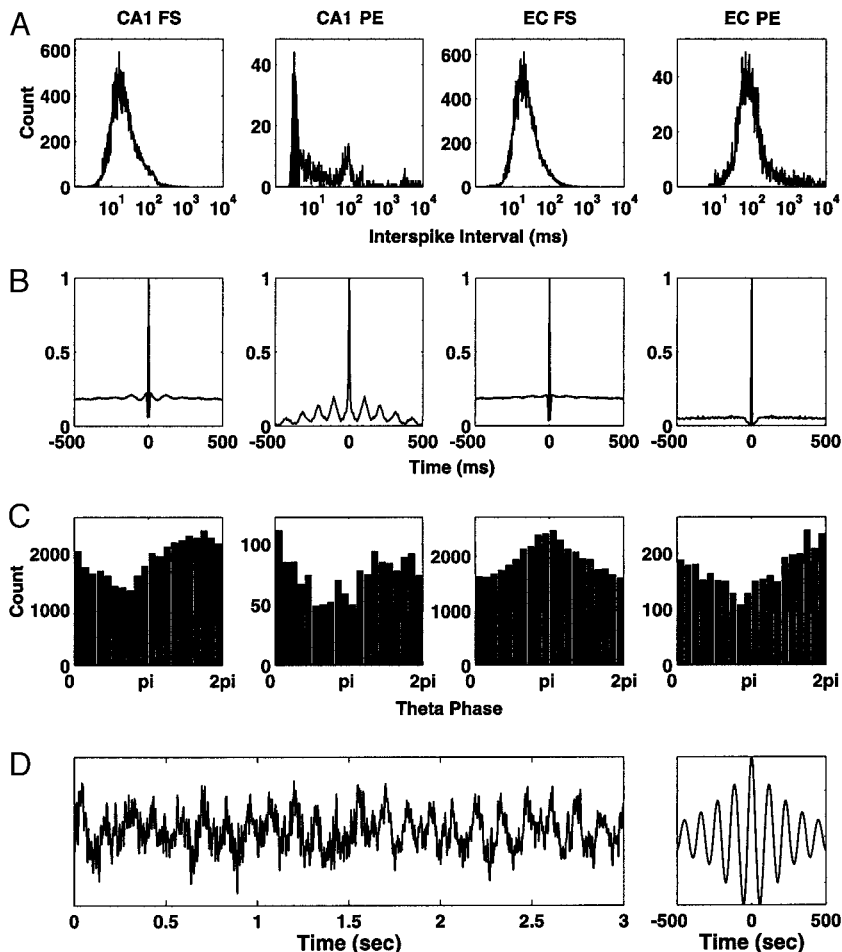


FIG. 5. Spiking properties of CA1 and EC units. *A*: interspike interval (ISI) distributions from a representative unit recorded in each region. CA1 and EC FS units had similar ISI distributions. CA1 PE unit ISI distributions showed the characteristic prevalence of short intervals, while these short interval spikes were generally not present in the ISIs of EC PE units that tended to have unimodal ISI distributions that peaked between 30 and 125 ms. *B*: normalized autocorrelation histograms for each of the units. Modulation by the theta rhythm is clearly visible in the histograms associated with the CA1 FS and PE units and is also apparent in histogram for the EC FS unit. *C*: histogram of number of spikes vs. theta phase for the theta rhythm taken from a deep EC electrode. While the degree of theta modulation apparent in the autocorrelation histograms varies substantially across the units, all of the units were strongly theta modulated. *D*: example raw electroencephalographic (EEG) trace (*left*) and autocorrelation of filtered signal (*right*). Theta is clearly visible in the raw EEG from the deep EC and in the autocorrelation.

essentially the same as those presented in Frank et al. (2000), so here we focus on the finding for FS units. The average proportion of the environment covered by a given unit's fields was not different among the FS units from different regions, but all FS units' fields tended to cover larger portions of the environment than PE units ( $P < 0.0001$ , Scheffé  $S$  test). Similarly, across regions the firing patterns of FS units carried similar amounts of position information. At the same time, all types of FS units' firing carried significantly less position information than the firing patterns of all types of PE units ( $P < 0.005$ , Wilcoxon rank-sum test used because the position information distributions were highly non-Gaussian). Once

again FS units from CA1 and the EC appear to have similar properties while PE units differed across region.

#### Prospective and retrospective coding

Table 2 shows the total number of units tested for prospective or retrospective firing. Examples of FS units from each region showing significant retrospective coding on the center arm are shown in Fig. 9A. Each plot shows the firing rate in each of the seven windows for paths including either the left or the right outside arm. The total numbers of units whose full GLM model was significant at  $P < 0.01$  are shown in Fig. 9B.

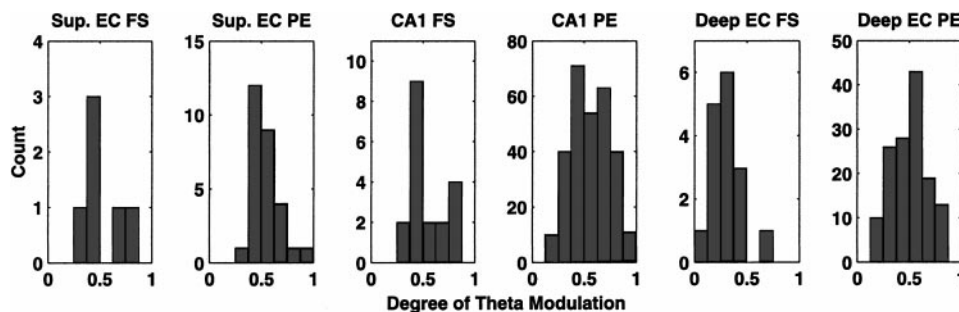


FIG. 6. Histograms of the distribution of the depth of theta modulation across unit type and region. Units of all types showed some degree of theta modulation, although deep EC FS units were significantly less theta modulated than superficial EC PE, CA1 PE and FS, and deep EC PE units (Scheffé  $S$  test,  $P < 0.01$ ). None of the other means were significantly different, indicating that theta modulation is prevalent throughout the EC and CA1. Note also that the distributions of superficial EC FS and CA1 FS units appear to be bimodal, suggesting that there may be different classes of interneurons with different degrees of theta modulation.

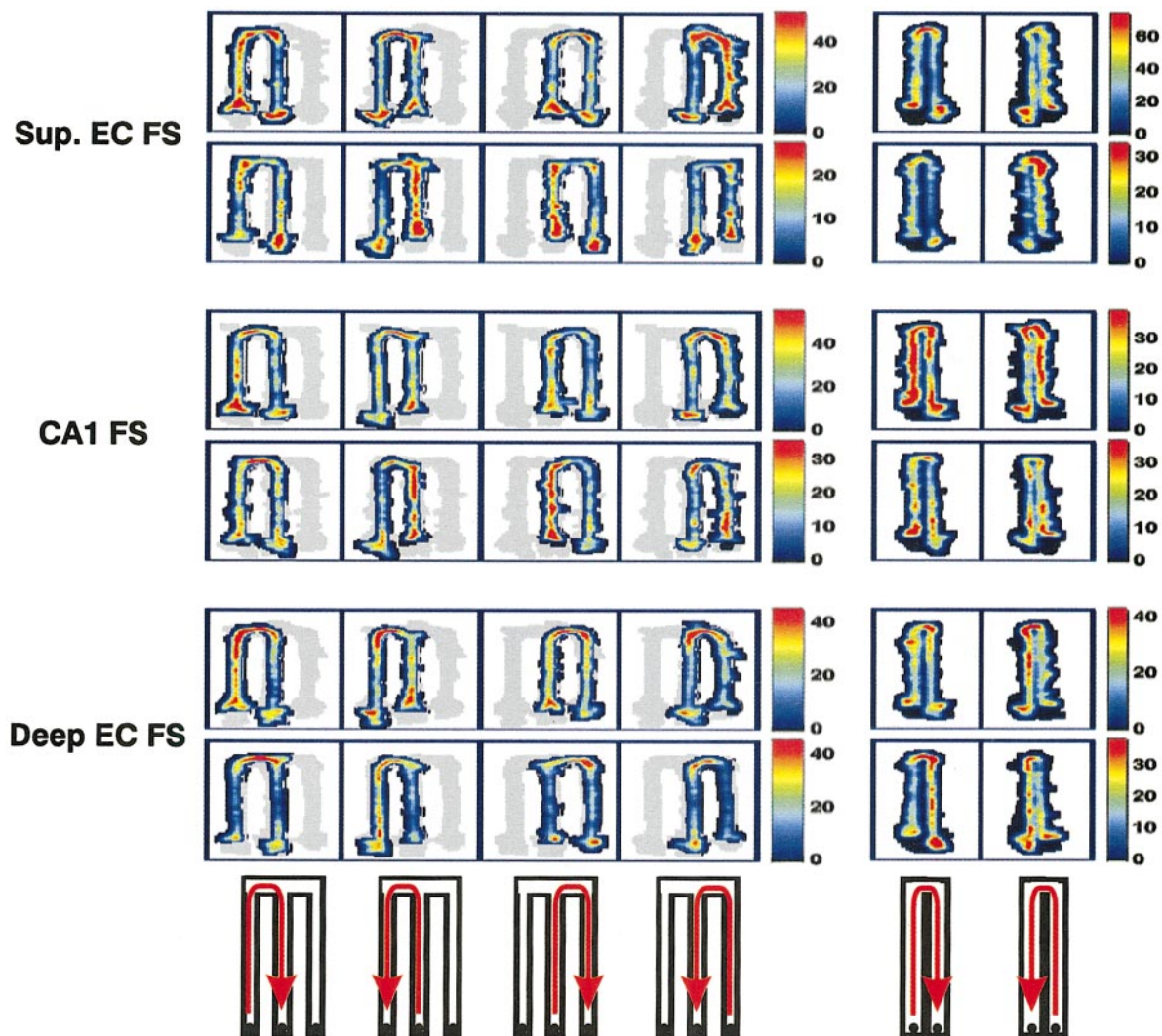


FIG. 7. Examples of FS unit firing patterns across the W- and U-track environment. Each row represents the firing of 1 unit that had a field in both the W- and U-tracks environments. Each panel within a row shows the firing rate of the unit across 1 path through the environment; *bottom*: the path the animal was on for each panel. FS units, while showing relatively little spatial specificity, showed clear areas of higher and lower firing rate. The peak of activity EC FS units, particularly deep EC FS units, was often in the same relative location across different paths even when those paths were in different environments, a phenomenon we have previously referred to as “path equivalence,” while the peak for CA1 FS units was generally in a different relative location on different paths. The bottom deep EC unit, for example, was preferentially active around the turns of both environments.

Overall, FS unit from CA1 and the deep EC showed retrospective coding with approximately the same frequency as their PE counterparts.

#### Path equivalence

The mean path equivalence coefficients (PECs) for comparisons of paths within the W track and for comparisons of paths between the W and U tracks are shown in Fig. 10. Earlier work had shown that deep EC units showed higher PECs than CA1 units (Frank et al. 2000). We determined that this relationship was maintained after classification. For the paths within the W track, the mean PEC for both deep EC FS and PE units was significantly higher than that than that of CA1 PE units ( $P < 0.002$ , Wilcoxon rank-sum test used because the distributions were non-Gaussian). The results for the W-U path comparison were generally similar in that both deep EC FS and PE units had significantly higher PECs than both CA1 FS and PE units.

None of the other comparisons yielded significant results ( $P > 0.005$ , criterion chosen to maintain family-wise error rate at  $P = 0.05$ ) although for both the W versus W and the W versus U comparisons, the  $P$  value for the comparison of deep EC FS and CA1 FS units was low ( $P < 0.06$  for W vs. W,  $P < 0.03$  for U vs. W). Relatively few superficial EC FS units were recorded from, so those units were not included in this analysis.

#### DISCUSSION

Our results suggest that the division of EC units into PE and FS subtypes is reasonable. The resulting PE and FS units had waveform widths and average rates that were in the same range as those reported in previous studies for neocortical units (Brumberg et al. 1996; McCormick et al. 1985; Rao et al. 1999; Simons 1978; Wilson et al. 1994), and the classifications were consistent across environments, suggesting that PE and FS units have consistently different average rates. We should also

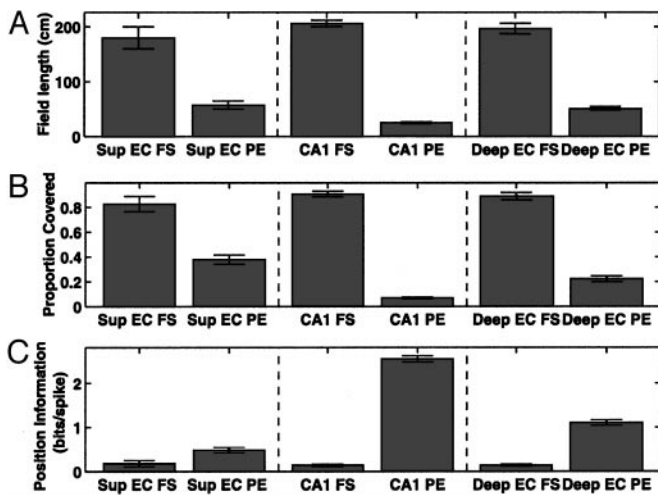


FIG. 8. Measures of spatial specificity for each type of unit from each region. *A*: average field length. The average field length of FS units' fields was about the same across regions and significantly larger than the average field length of all PE units. In addition, EC PE units had longer fields than CA1 PE units (all  $P < 0.0001$ , Scheffé  $S$  test). *B*: the average proportion of the environment covered by units' fields. FS units' fields covered significantly larger fractions of the environment than those of PE units. *C*: position information. Not surprisingly, the mean amount of position information followed similar trends as the field size and proportion of the environment covered by fields in that FS units firing carried, on average, less position information than that of PE units ( $P < 0.05$  for superficial EC,  $P < 0.0001$  for CA1 and deep EC PE units, Wilcoxon rank-sum test). The relationships among PE units were the same as those presented in our previous manuscript (Frank et al. 2000).

note that the total distribution of average firing rates was generally similar to that presented by Barnes et al. (1990) and Mizumori et al. (1992). At the same time, the overall average rate for superficial EC cells reported by Quirk et al. (1992) was  $7.1 \pm 9.0$  Hz, a rate much higher than that of EC PE units in our study, suggesting that a relatively large proportion of the units they recorded from may have been FS units.

In addition, the cross-correlation analyses revealed that, for both CA1 and the deep EC, PE and FS units recorded simultaneously on the same tetrode were much more likely to show a strong short-time cross-correlation than pairs of PE units. That also supports our contention that our division of units into PE and FS subtypes reflects an actual difference in the cells we recorded from; if the division was not valid, we would not expect to see differences in the likelihood of a significant short-time cross-correlation. Our finding is consistent with the results of Csicsvari et al. (1998), who demonstrated that the

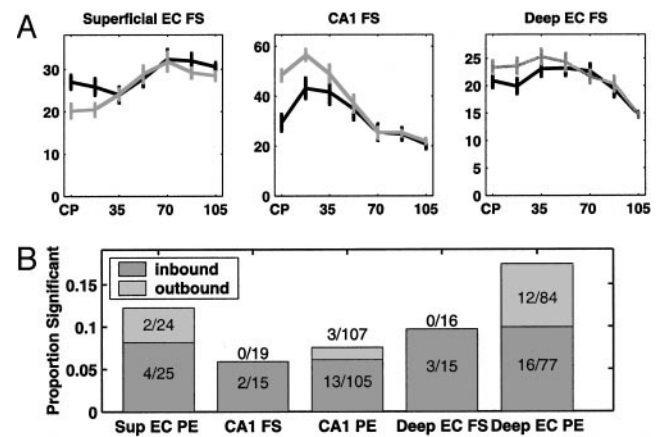


FIG. 9. Prospective and retrospective coding across regions and unit types. *A*: FS units from each region showing retrospective coding. Each plot shows the firing rate of the unit in each of the 7 windows on the center arm on both paths involving the left arm (black line) and the right arm (gray line) and the error bars represent 1 SE. CP, choice point. FS units did show retrospective activity, usually relatively close to the CP, and while the associated firing rate differences were small, they were clearly significant. *B*: the number of units of each type from each region showing prospective (light gray bars) or retrospective (darker gray bars) activity based on the full GLM model with either a significant cutoff at  $P < 0.01$ . One of 3 superficial EC FS units showed significant retrospective coding, but as only 3 units were not eliminated from the analysis, the proportions are not meaningful and so superficial EC FS units were omitted from the proportion significant analysis. For all unit types shown, a greater number of both PE units showed retrospective coding than would be expected by chance. In addition, for PE but not FS units, a greater number showed prospective coding than would be expected by chance, although the number of FS units examined was relatively small, so we cannot conclude that FS units do not show prospective coding. The number of units showing prospective coding was inhomogeneous ( $P < 0.01$ , logistic regression), suggesting that prospective coding is most prevalent in the deep EC. Note that the criteria for determining that a cell shows prospective or retrospective coding are very restrictive, and the actual proportion of cells showing some form of prospective or retrospective activity may be closer to 50% (see Table 2).

firing of CA1 theta (FS) units was strongly coupled to that of individual CA1 pyramidal (PE) units. Thus our results suggest that in both CA1 and the deep EC, there are strong monosynaptic connections between PE and FS units.

#### Spike train properties

Overall, the interspike interval distributions, autocorrelations, and proportion of spikes associated with bursts for superficial EC, CA1, and deep EC FS units were similar, suggesting that the hippocampal and EC inhibitory cells have

TABLE 2. Units used in the prospective and retrospective coding analyses

	Superficial EC FS	Superficial EC PE	CA1 FS	CA1 PE	Deep EC FS	Deep EC PE
Total tested	11	49	38	218	32	164
Number significant	9	11	17	79	19	77
P/D/V eliminated	5	4	11	48	13	47
Inconsistent eliminated	3	0	4	6	1	3

The first row shows the number of units tested from each region. Note that a unit that had a field on the center arm of the W track in both inbound and outbound directions was counted as two units, one for each direction. The second row shows the number of units where the single-window GLM analysis was significant in at least one window, indicating the presence of prospective or retrospective coding. Overall, between 22 and 82% of the units showed some prospective or retrospective coding, indicating that a large proportion of CA1 and EC units fire at different rates depending on the animal's past or intended future position. The third row shows the number of units that were then excluded from the analysis because the prospective or retrospective coding was associated with lateral position differences (P), head differences  $>10^\circ$  (D), or velocity differences  $>5$  cm/sec (V). The fourth row gives the number of units that were eliminated from the analysis because they showed inconsistent prospective or retrospective coding, where the firing rate was higher for a path involving the left arm of the W track in one window and higher for a path involving the right arm in a different window.

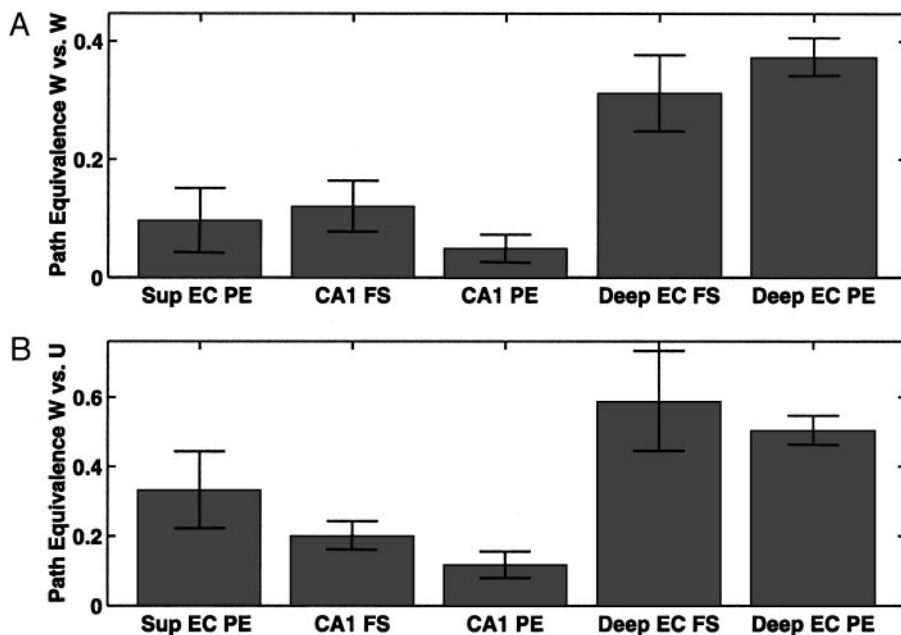


FIG. 10. The average path equivalence coefficients. Path equivalence, a measure of the extent to which a unit was active in the same relative location along multiple paths through either one environment (W versus W) or across environments (W versus U) was significantly higher for Deep EC FS and PE units than for CA1 FS and PE units. That suggests that while the spatial specificity of FS and PE units is very different, the relationship of their activity to the geometry of the track and to the behavior of the animal is similar.

similar firing properties. The spike train properties of PE units from CA1 and the EC, on the other hand, were very different, as CA1 PE units frequently fired in bursts while EC PE units seldom fired in bursts. As bursts are thought to be related to the induction of plasticity both pre- and postsynaptically in the hippocampus (Lisman 1997; Thomas et al. 1998), that suggests that there may be differences in the nature of the induction of plasticity in CA1 as compared with the EC.

#### Theta modulation

We found that the firing of both PE and FS units from all regions were theta modulated, although deep EC FS units tended to be less strongly modulated than other types of units. That result is consistent with previous data from the *in vitro* preparation documenting subthreshold membrane oscillations at the frequency of the theta rhythm in both superficial and deep EC units (Hamam et al. 2000; Schmitz et al. 1998) and with results from the intact animal where theta modulated units have been found in the superficial and deep EC (Alonso and Garcia-Austt 1987b; Jeffery et al. 1995; Stewart et al. 1992). At the same time, we should note that Chrobak and Buzsaki (1994) reported that while the superficial EC units they recorded from were theta modulated, the deep EC units were not.

#### Spatial firing properties

Just as FS units from the superficial EC, CA1, and the deep EC had generally similar spike train characteristics, these units also had similar spatial firing properties. FS units tended to have long fields that covered a large proportion of the environment, and the firing of these units contained relatively little position information, a result consistent with previous findings for CA1 FS units (Kubie et al. 1990; McNaughton et al. 1983) and, more generally, with findings from FS units in rat sensory cortex (Brumberg et al. 1996; Simons 1978).

Overall, the results from the spike train and spatial firing properties suggest that FS units from the superficial EC, CA1, and the deep EC are generally similar to one another both in

terms of the structure of their spike trains and in terms of simple measures of spatial receptive field properties. FS units tended to have different properties than PE units, and PE units from CA1 tended to be quite different from PE units from the EC, in terms of their spike train properties and the degree of spatial specificity seen in their firing. Those results suggest that FS units from CA1 and the EC may have similar physiological properties while PE units from these regions differ substantially.

#### Prospective/retrospective coding and path equivalence

While FS and PE units differed substantially in terms of their spike train characteristics and the measures of spatial specificity discussed in the preceding text, the two "higher-order" analyses of spatial firing properties, prospective/retrospective coding, and path equivalence, yielded more similar results for PE and FS units from each region. Both PE and FS units showed retrospective coding, and the proportion of PE and FS units showing this property were similar in CA1 and the deep EC. Prospective coding was observed only in PE units and was most prevalent in the deep EC, but as the numbers of FS units were relatively small, we cannot conclude that FS units do not show prospective coding. As such, FS units appear to be as likely as PE units to fire at a different rate in the same location depending on the animal's past location. The activity of FS units can therefore reflect the relationships between the animal's position and the trajectory through the environment. Furthermore, deep EC PE and FS units tended to show strongly path equivalent firing while CA1 PE and FS units tended to show less path equivalent firing. These results are generally consistent with those of Rao et al. (1999), who found that FS activity in the primate prefrontal cortex also reflected complex stimulus attributes. The most obvious explanation for the presence of these higher-order spatial firing properties in the firing of FS units is the previously discussed coupling between PE and FS units.

### General conclusions

The EC, despite its prominent anatomical relationships with the hippocampus, is poorly understood. By simultaneously recording from PE and FS units in CA1 and the EC, we have directly compared the firing properties of these units. We found that FS units from CA1 and the EC tended to have similar interspike interval histograms and levels of spatial specificity. At the same time, the depth of theta modulation apparent in their firing patterns differed in that deep EC FS units were less theta modulated than superficial EC or CA1 FS units. In addition, deep EC FS units showed a stronger tendency to exhibit the higher-order spatial firing properties of retrospective coding and path equivalence than their CA1 counterparts. These results suggest that these putative interneurons from CA1 and the EC show both similarities that may reflect common cellular or physiological characteristics as well as differences that may reflect the computations that are performed in each region.

The authors thank C. Lena, A. Nathe, and M. Quirk for comments on an earlier version of the manuscript.

This work was supported by the Defense Advanced Research Projects Agency, the Office of Naval Research, the Center for Learning and Memory at MIT, and National Institute of Mental Health Grants MH-59733, MH-61637, and MH-58880.

### REFERENCES

- ALONSO A AND GARCIA-AUSTT E. Neuronal sources of theta rhythm in the entorhinal cortex of the rat. I. Laminar distribution of theta field potentials. *Exp Brain Res* 67: 493–501, 1987a.
- ALONSO A AND GARCIA-AUSTT E. Neuronal sources of theta rhythm in the entorhinal cortex of the rat. II. Phase relations between unit discharges and theta field potentials. *Exp Brain Res* 67: 502–509, 1987b.
- AMARAL DG AND WITTER MP. Hippocampal formation. In: *The Rat Nervous System*, edited by Paxinos C. New York: Academic, 1995, p. 443–493.
- BARNES CA, MCNAUGHTON BL, MIZUMORI SJ, LEONARD BW, AND LIN LH. Comparison of spatial and temporal characteristics of neuronal activity in sequential stages of hippocampal processing. *Prog Brain Res* 83: 287–300, 1990.
- BEHRMANN DL, BRESNAHAN JC, AND BEATTIE MS. Modeling of acute spinal cord injury in the rat: neuroprotection and enhanced recovery with methylprednisolone U-74006F and YM-14673. *Exp Neurol* 126: 61–75, 1994.
- BRILLINGER DR. Estimation of the second-order intensities of a bivariate stationary point process. *J Roy Statist Soc B* 38: 60–66, 1976.
- BRUMBERG JC, PINTO DJ, AND SIMONS DJ. Spatial gradients and inhibitory summation in the rat whisker barrel system. *J Neurophysiol* 76: 130–140, 1996.
- BUZSAKI G AND EIDELBERG E. Phase relations of hippocampal projection cells and interneurons to theta activity in the anesthetized rat. *Brain Res* 266: 334–339, 1983.
- BUZSAKI G, PENTTONEN M, NADASY Z, AND BRAGIN A. Pattern and inhibition-dependent invasion of pyramidal cell dendrites by fast spikes in the hippocampus in vivo. *Proc Natl Acad Sci USA* 93: 9921–9925, 1996.
- CHO YH AND JAFFARD R. The entorhinal cortex and a delayed non-matching-to-place task in mice: emphasis on preoperative training and presentation procedure. *Eur J Neurosci* 6: 1265–1274, 1994.
- CHO YH AND KESNER RP. Involvement of entorhinal cortex or parietal cortex in long-term spatial discrimination memory in rats: retrograde amnesia. *Behav Neurosci* 110: 436–442, 1996.
- CHROBAK JJ AND BUZSAKI G. Selective activation of deep layer (V–VI) retro-hippocampal cortical neurons during hippocampal sharp waves in the behaving rat. *J Neurosci* 14: 6160–6170, 1994.
- CHROBAK JJ AND BUZSAKI G. Gamma oscillations in the entorhinal cortex of the freely behaving rat. *J Neurosci* 18: 388–398, 1998.
- CSCSIVARI J, HIRASE H, CZURKO A, MAMIYA A, AND BUZSAKI G. Reliability and state dependence of pyramidal cell-interneuron synapses in the hippocampus: an ensemble approach in the behaving rat. *Neuron* 21: 179–189, 1998.
- CSCSIVARI J, HIRASE H, CZURKO A, MAMIYA A, AND BUZSAKI G. Oscillatory coupling of hippocampal pyramidal cells and interneurons in the behaving rat. *J Neurosci* 19: 274–287, 1999.
- FOX SE AND RANCK JBJ. Electrophysiological characteristics of hippocampal complex-spike cells and theta cells. *Exp Brain Res* 41: 399–410, 1981.
- FRANK LM, BROWN EN, AND WILSON MA. Trajectory encoding in the hippocampus and entorhinal cortex. *Neuron* 27: 169–178, 2000.
- GARCIA-SANCHEZ JL, BUNO W JR, FUENTES J, AND GARCIA-AUSTT E. Non-rhythmic hippocampal units, theta rhythm and afferent stimulation. *Brain Res Bull* 3: 213–219, 1978.
- HAGAN JJ, VERHEIJCK EE, SPIGT MH, AND RUIGT GS. Behavioural and electrophysiological studies of entorhinal cortex lesions in the rat. *Physiol Behav* 51: 255–266, 1992.
- HAMAM BN, KENNEDY TE, ALONSO A, AND AMARAL DG. Morphological and electrophysiological characteristics of layer V neurons of the rat medial entorhinal cortex. *J Comp Neurol* 418: 457–472, 2000.
- HOLSCHER C AND SCHMIDT WJ. Quinolinic acid lesion of the rat entorhinal cortex pars medialis produces selective amnesia in allocentric working memory (WM), but not in egocentric WM. *Behav Brain Res* 63: 187–194, 1994.
- IZQUIERDO I AND MEDINA JH. Role of the amygdala, hippocampus and entorhinal cortex in memory consolidation and expression. *Braz J Med Biol Res* 26: 573–589, 1993.
- IZQUIERDO I, QUILLFELDT JA, ZANATTA MS, QUEVEDO J, SCHAEFFER E, SCHMITZ PK, AND MEDINA JH. Sequential role of hippocampus and amygdala, entorhinal cortex and parietal cortex in formation and retrieval of memory for inhibitory avoidance in rats. *Eur J Neurosci* 9: 786–793, 1997.
- JARRARD LE. On the role of the hippocampus in learning and memory in the rat. *Behav Neural Biol* 60: 9–26, 1993.
- JEFFERY KJ, DONNETT JG, AND O'KEEFE J. Medial septal control of theta-correlated unit firing in the entorhinal cortex of awake rats. *Neuroreport* 6: 2166–2170, 1995.
- JOHNSON DL AND KESNER RP. The effects of lesions of the entorhinal cortex and the horizontal nucleus of the diagonal band of Broca upon performance of a spatial location recognition task. *Behav Brain Res* 61: 1–8, 1994.
- JUNG MW AND MCNAUGHTON BL. Spatial selectivity of unit activity in the hippocampal granular layer. *Hippocampus* 3: 165–182, 1993.
- KUBIE JL, MULLER RU, AND BOSTOCK E. Spatial firing properties of hippocampal theta cells. *J Neurosci* 10: 1110–1123, 1990.
- KYRIAZI HT, CARVELL GE, BRUMBERG JC, AND SIMONS DJ. Quantitative effects of GABA and bicuculline methiodide on receptive field properties of neurons in real and simulated whisker barrels. *J Neurophysiol* 75: 547–560, 1996.
- LISMAN JE. Bursts as a unit of neural information: making unreliable synapses reliable [see comments]. *Trends Neurosci* 20: 38–43, 1997.
- MCCORMICK DA, CONNORS BW, LIGHTHALL JW, AND PRINCE DA. Comparative electrophysiology of pyramidal and sparsely spiny stellate neurons of the neocortex. *J Neurophysiol* 54: 782–806, 1985.
- MCHUGH TJ, BLUM KI, TSJEN JZ, TONEGAWA S, AND WILSON MA. Impaired hippocampal representation of space in CA1-specific NMDAR1 knockout mice [see comments]. *Cell* 87: 1339–1349, 1996.
- MCNAUGHTON BL, BARNES CA, AND O'KEEFE J. The contributions of position, direction, and velocity to single unit activity in the hippocampus of freely-moving rats. *Exp Brain Res* 52: 41–49, 1983.
- MIZUMORI SJ, WARD KE, AND LAVOIE AM. Medial septal modulation of entorhinal single unit activity in anesthetized and freely moving rats. *Brain Res* 570: 188–197, 1992.
- MULLER R. A quarter of a century of place cells. *Neuron* 17: 813–822, 1996.
- MULLER RU, BOSTOCK E, TAUBE JS, AND KUBIE JL. On the directional firing properties of hippocampal place cells. *J Neurosci* 14: 7235–7251, 1994.
- NAGAHARA AH, OTTO T, AND GALLAGHER M. Entorhinal-perirhinal lesions impair performance of rats on two versions of place learning in the Morris water maze. *Behav Neurosci* 109: 3–9, 1995.
- O'KEEFE J AND DOSTROVSKY J. The hippocampus as a spatial map. Preliminary evidence from unit activity in the freely-moving rat. *Brain Res* 34: 171–175, 1971.
- O'KEEFE J AND NADEL L. *The Hippocampus as a Cognitive Map*. London, UK: Oxford Univ. Press, 1978.
- PERKEL DH, GERSTEIN GL, AND MOORE GP. Neuronal spike trains and stochastic point processes. II. Simultaneous spike trains. *Biophys J* 7: 419–440, 1967.

- QUIRK GJ, MULLER RU, KUBIE JL, AND RANCK JB JR. The positional firing properties of medial entorhinal neurons: description and comparison with hippocampal place cells. *J Neurosci* 12: 1945–1963, 1992.
- QUIRK MC AND WILSON MA. Interaction between spike waveform classification and temporal sequence detection. *J Neurosci Methods* 94: 41–52, 1999.
- RAO SG, WILLIAMS GV, AND GOLDMAN-RAKIC PS. Isodirectional tuning of adjacent interneurons and pyramidal cells during working memory: evidence for microcolumnar organization in PFC. *J Neurophysiol* 81: 1903–1916, 1999.
- RASMUSSEN M, BARNES CA, AND MCNAUGHTON B. A systematic test of cognitive mapping, working-memory, and temporal discontinuity theories of hippocampal function. *Psychobiology* 17: 335–348, 1989.
- SCHMITZ D, GLOVELI T, BEHR J, DUGLADZE T, AND HEINEMANN U. Subthreshold membrane potential oscillations in neurons of deep layers of the entorhinal cortex. *Neuroscience* 85: 999–1004, 1998.
- SHARP PE. Subicular cells generate similar spatial firing patterns in two geometrically and visually distinctive environments: comparison with hippocampal place cells. *Behav Brain Res* 85: 71–92, 1997.
- SIMONS DJ. Response properties of vibrissa units in rat SI somatosensory neocortex. *J Neurophysiol* 41: 798–820, 1978.
- SKAGGS WE, MCNAUGHTON BL, GOTHARD K, AND MARKUS E. An information-theoretic approach to deciphering the hippocampal code. In: *Advances in Neural Information Processing 5*, edited by Hanson SJ, Cowan JD, and Giles CL. San Mateo, CA: Morgan Kaufman, 1993, p. 1030–1037.
- STEWART M, QUIRK GJ, BARRY M, AND FOX SE. Firing relations of medial entorhinal neurons to the hippocampal theta rhythm in urethane anesthetized and walking rats. *Exp Brain Res* 90: 21–28, 1992.
- SUTHERLAND RJ, McDONALD RJ, HILL CR, AND RUDY JW. Damage to the hippocampal formation in rats selectively impairs the ability to learn cue relationships [published erratum appears in *Behav Neural Biol* 54: 211–212, 1990]. *Behav Neural Biol* 52: 331–356, 1989.
- SWADLOW HA. Influence of VPM afferents on putative inhibitory interneurons in S1 of the awake rabbit: evidence from cross-correlation, microstimulation, and latencies to peripheral sensory stimulation. *J Neurophysiol* 73: 1584–1599, 1995.
- SWADLOW HA, BELOOZEROVA IN, AND SIROTA MG. Sharp, local synchrony among putative feed-forward inhibitory interneurons of rabbit somatosensory cortex. *J Neurophysiol* 79: 567–582, 1998.
- THOMAS MJ, WATABE AM, MOODY TD, MAKHINSON M, AND O'DELL TJ. Postsynaptic complex spike bursting enables the induction of LTP by theta frequency synaptic stimulation. *J Neurosci* 18: 7118–7126, 1998.
- VNEK N, GLEASON TC, KROMER LF, AND ROTHBLAT LA. Entorhinal-hippocampal connections and object memory in the rat: acquisition versus retention. *J Neurosci* 15: 3193–3199, 1995.
- WHISHAW IQ AND TOMIE JA. Acquisition and retention by hippocampal rats of simple, conditional, and configural tasks using tactile and olfactory cues: implications for hippocampal function. *Behav Neurosci* 105: 787–797, 1991.
- WILSON FA, O'SCALAIDHE SP, AND GOLDMAN-RAKIC PS. Functional synergism between putative gamma-aminobutyrate-containing neurons and pyramidal neurons in prefrontal cortex. *Proc Natl Acad Sci USA* 91: 4009–4013, 1994.
- WITTER MP, VAN HOESEN GW, AND AMARAL DG. Topographical organization of the entorhinal projection to the dentate gyrus of the monkey. *J Neurosci* 9: 216–228, 1989.